Quantum confinement in EuO heterostructures

Günther M. Prinz, Timm Gerber, Axel Lorke, and Martina Müller

Citation: Applied Physics Letters **109**, 202401 (2016); doi: 10.1063/1.4966223
View online: http://dx.doi.org/10.1063/1.4966223
View Table of Contents: http://scitation.aip.org/content/aip/journal/apl/109/20?ver=pdfcov
Published by the AIP Publishing

Quantum confinement in EuO heterostructures

Günther M. Prinz,[1] Timm Gerber,[2] Axel Lorke,[1] and Martina Müller[1,2,a)]
[1]*Fakultät für Physik and CENIDE, Universität Duisburg-Essen, D-47048 Duisburg, Germany*
[2]*Peter Grünberg Institut (PGI-6), Forschungszentrum Jülich GmbH, D-52428 Jülich, Germany*

(Received 9 May 2016; accepted 14 October 2016; published online 14 November 2016)

Quantum wells are created from ultrathin single-crystalline EuO layers to study the evolution of the optical band gap down to the single nanometer regime. We find that the EuO band gap is indirect—independent of quantum well thickness—and increases from 1.19 eV for bulk-like ($d = 32$ nm) to ≈1.4 eV in the ultrathin films ($d = 1.1$ nm). The observed band-gap widening is a clear sign of a quantum confinement effect, which can be used to control and modify the band gap in EuO-based all-oxide heterostructures. *Published by AIP Publishing.*
[http://dx.doi.org/10.1063/1.4966223]

Recent years have witnessed significant advances in layer-by-layer growth of oxide thin films with atomic-scale precision.[1] The fabrication of artificial heterostructures has enabled interface and size control of complex oxide materials, for which unique phenomena with no bulk analogues have been demonstrated.[2,3] Going beyond oxide surfaces and interfaces, the next simplest heterostructure is a quantum well (QW). In a QW, the charge carriers are confined along one dimension—typically the growth direction—due to the large band-gap discontinuities at the interfaces. Quantum size effects make it possible to tailor the effective band gap of the oxide material and control its optical and electronic properties in emerging applications—in terms of quality that were thought to be unique to semiconductors.

The basic idea of quantum confinement—using potential gradients caused by band offsets or band bending—applies to complex oxides just as to conventional semiconductors, but the physics is much richer. In metal oxides, confined electrons are subject to strong electron-electron interactions leading to a variety of physical phenomena that can be accessed, modified and controlled in quantum wells.[4] For example, using oxides with intrinsic magnetic order allows to combine spin-related phenomena with optoelectronic applications.[5]

In this context, europium monoxide (EuO) shows remarkable properties: It is a strong ferromagnet with a Curie temperature of $T_C = 69$ K and a bulk magnetic moment of $7\mu_B$.[6] EuO undergoes a large magnetization-driven insulator-to-metal transition below T_C, displays large magneto-optical effects[7] (Kerr rotation ~7.1°), and can generate up to 100% spin-polarized electron currents if employed as a magnetic tunnel barrier.[8–10]

The electronic configuration of europium monoxide is [Xe] $4f^7 5d^0 6s^0$ for the Eu^{2+} ion and [He] $2s^2 2p^6$ for the O^{2-} ion. The optical spectrum is dominated by transitions from the $4f$ valence band (VB) orbitals to the $5d - 6s$ conduction band (CB) across a band gap of $E_{gap} \approx 1.12$ eV.[11] Interestingly, even fundamental optical properties, such as the nature of the band gap—direct or indirect—remain a subject of debate and often have to rely on the works published many decades ago before high-quality EuO thin films became available.[6,11]

Recent advances in the growth of EuO[12] now make it possible to study optoelectronic properties down to the few atomic layer limit. In this work, the choice of suitable substrate and capping materials depends not only on their good transparency up to the UV range but also on the ability to realize all-oxide multilayers with heteroepitaxial order. We employ yttria-stabilized zirconia (YSZ) and MgO with the large band gaps of 7.8 eV and 4.2 eV, respectively, and make use of the virtually identical lattice constants of YSZ and EuO ($a_{YSZ} = a_{EuO} = 5.14$ Å, see Fig. 1 for schematics of the resulting atomic arrangement and band alignment). Furthermore, EuO is thermodynamically stable in contact with YSZ,[13] which allows the well defined heteroepitaxial growth of EuO layers with monolayer precision, while maintaining its intriguing physical properties.

To investigate possible size effects, EuO thin films were grown in an ultrahigh vacuum MBE system with a residual gas pressure $p < 2 \times 10^{-10}$ mbar. The substrates were (001)-oriented YSZ (composition $Zr_{0.87}Y_{0.13}O_{1.935}$, epi-polished on both sides). Prior to thin film growth, the substrates were

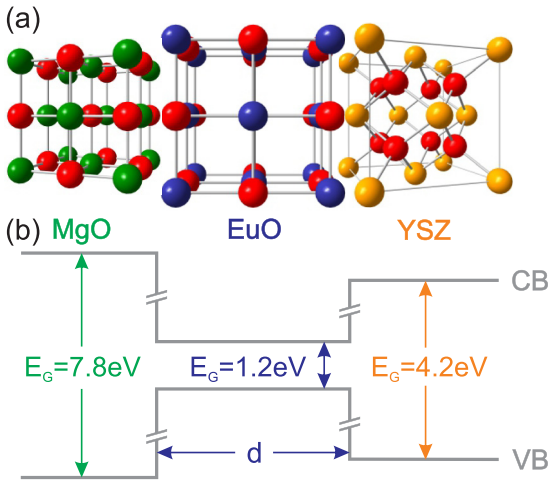

FIG. 1. (a) Crystal structures and stacking of the MgO/EuO/YSZ heterostructure. (b) Electronic structure of the all-oxide quantum well. Valence band (VB) and conduction band (CB) are drawn as gray lines. Interrupted lines indicate that exact values of the band offsets are not known.

a)Author to whom correspondence should be addressed. Electronic mail: mart.mueller@fz-juelich.de

annealed in vacuum at $T_S = 600\,^{\circ}\mathrm{C}$ for $t = 2\,\mathrm{h}$ with an oxygen pressure of $p_{O_2} = 1 \times 10^{-7}$ mbar.[14]

Stoichiometric EuO was synthesized by evaporating 99.99% pure Eu with a deposition rate of 0.13 Å/s from a low-temperature effusion cell in an O_2 atmosphere. Using customized gas inlets, the oxygen gas was evenly distributed to the sample surface and to a quadrupole mass spectrometer, which was used to carefully control the partial O_2 pressure. The substrate temperature was set to 500 °C during growth.

The EuO films were grown using the distillation method.[12,15] Growth was always initiated by exposing the sample to Eu metal flux. Subsequently, the O_2 flux was ramped to the desired value within ≈30 s. A flux ratio of $J_{Eu}/J_O \approx 1.1$ was used to ensure the correct stoichiometry by re-evaporation of excess Eu metal. The samples were analyzed *in situ* by reflection high-energy electron diffraction (RHEED), low-energy electron diffraction (LEED), and X-ray photoemission spectroscopy (XPS, Al-K_α). Prior to *ex situ* measurements, the samples were capped with an MgO layer ($d = 10\,\mathrm{nm}$) to prevent further oxidation of the metastable EuO films in air. MgO was e-beam evaporated at a rate of 0.2 Å/s with the sample at room temperature. Additional structural analysis was carried out *ex situ* by X-ray diffraction (XRD) using a Philips X'Pert four-circle diffractometer. X-ray reflectivity (XRR) was used to determine the EuO growth rate, layer thickness d and surface roughness R. The thickness of the EuO layers was cross-checked by measuring their saturation moment with a Quantum Design superconducting quantum interference device (SQUID) magnetometer.

Fig. 2(a) shows the RHEED patterns of the YSZ substrate (top), the EuO layer ($d = 32\,\mathrm{nm}$, middle), and the MgO capping layer (bottom). As expected, the reflections of YSZ and EuO are observed at the same positions on the RHEED screen, since the lattice constants of YSZ and EuO are virtually identical ($a_{YSZ} = a_{EuO} = 5.14$ Å). The first order reflections of the EuO film are narrow streaks indicative of a flat and well ordered surface. After deposition of the MgO capping layer, broad spots of a transmission pattern are observed. Thus, the MgO layer is also epitaxial but not as flat and ordered as the EuO layer. Comparing the position of the MgO spots with the EuO film (or YSZ substrate) yields $a_{MgO} = (4.2 \pm 0.1)$ Å, consistent with the bulk reference value $a_{MgO} = 4.21$ Å. Thus, the MgO layer is fully relaxed and an influence of strain on the EuO layer is not present.

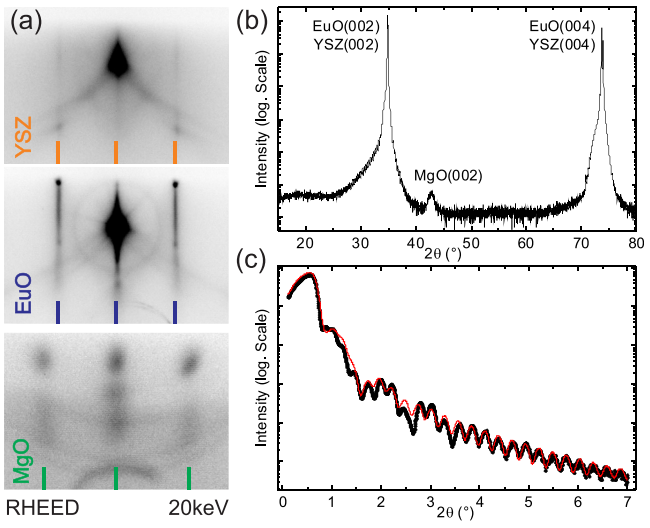

FIG. 2. (a) Inverted contrast RHEED pattern (20 keV) of the YSZ substrate (top), the EuO layer ($d = 32\,\mathrm{nm}$, middle), and the MgO capping layer (bottom). Zero and first order reflections are indicated. (b) X-ray diffraction of the same heterostructure showing only EuO/YSZ and MgO reflections. (c) X-ray reflectivity data (black) and fit (red). Kiessig fringes are clearly visible over the whole angular range.

Fig. 2(b) shows XRD data of the same heterostructure. Only the EuO/YSZ and MgO reflections are observed, indicating that the EuO layer is single-crystalline and also confirming the epitaxial growth of the MgO capping layer. Fig. 2(c) shows the corresponding XRR measurement (black dots). Using a fit model based on the Parratt recursion (red line), the thickness d of the layers and roughness R of the interfaces are derived as $d_{EuO} = (31.8 \pm 0.1)\,\mathrm{nm}$, $d_{MgO} = (9.2 \pm 0.5)\,\mathrm{nm}$, $R_{EuO} = (0.4 \pm 0.1)\,\mathrm{nm}$ and $R_{MgO} = (1.4 \pm 0.1)\,\mathrm{nm}$.

Optical transmission measurements were carried out with a Bruker IFS 66v/S Fourier transform infrared spectrometer. For the spectral region of interest, i.e. $h\nu > 1\,\mathrm{eV}$, we used a Si photo-diode detector and a quartz glass beam splitter. The transmission I of each sample was recorded and normalized using a spectrum of a reference sample (I_0), grown under identical conditions, but without an EuO layer.

Fig. 3(a) shows the extinction coefficient α as given by Lambert-Beer's formula $\alpha = -\ln(\frac{I}{I_0})/d$, where d is the thickness of the EuO layer. For better comparison of the samples with different d, the data were scaled to match the extinction coefficient of the sample with $d = 32\,\mathrm{nm}$ thickness. As can be seen from Fig. 3(a), with decreasing EuO layer thickness, the absorption edge clearly shifts towards higher energies. This is a strong indication of band-gap tuning by quantum confinement.[16]

First, we address the fundamental question whether the EuO band gap is of direct or indirect nature. In a previous work by Güntherodt *et al.*,[11] a direct band gap was assumed to evaluate the absorption data. More recent experimental and theoretical studies, however, have indicated that the EuO band gap is indirect.[17–20]

In general, the absorption coefficient α near the optical gap energy E_{opt} follows the relation[21]

$$\alpha \cdot h\nu \propto (h\nu - E_{opt})^f, \tag{1}$$

with the photon energy $h\nu$. For a direct gap $f = 1/2$, whereas $f = 2$ for an indirect gap.[22] The inset in Fig. 3(b) exemplarily shows in a double-logarithmic representation the two possible fit functions in comparison with the experimental data for $d = 1.1\,\mathrm{nm}$. Obviously, the fit with exponent $f = 2$ (red line) agrees very well near the onset of absorption, whereas the direct gap absorption (blue line with slope $f = 1/2$) does not even show a qualitative agreement. This finding is true for all investigated samples with layer thicknesses between $d = 1.1\,\mathrm{nm}$ and 32 nm and strongly confirms that EuO has an indirect band gap – independent of the film thickness.

In order to evaluate the band-gap shift quantitatively, the square root of the product of the extinction coefficient

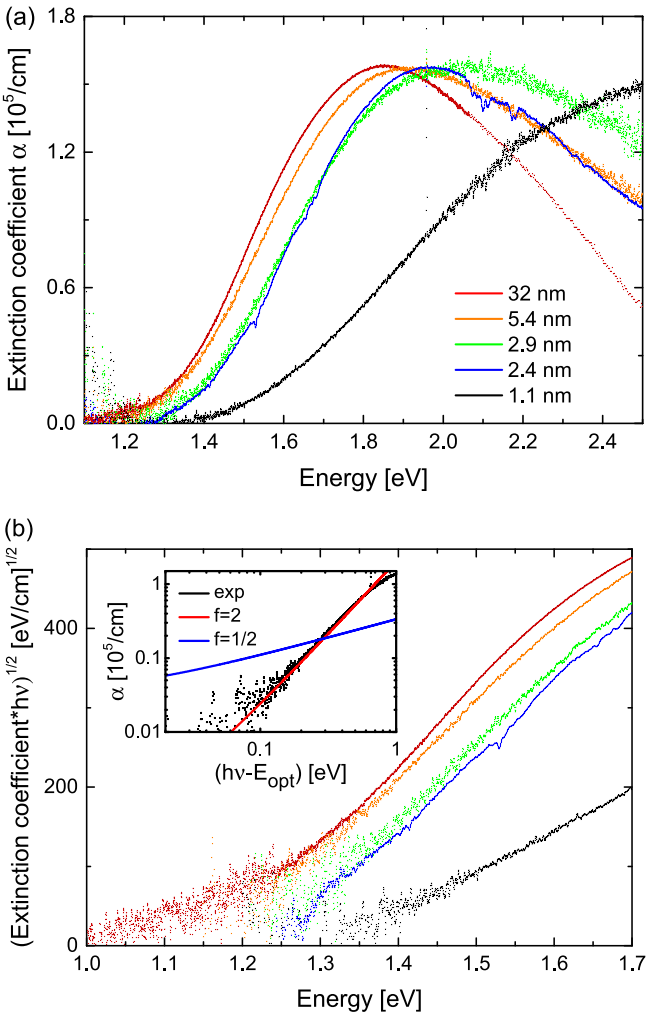

FIG. 3. (a) Extinction coefficient α of EuO thin films with thicknesses between $d = 1.1$ nm and 32 nm. Data was scaled to match α of the 32 nm sample for better comparison. A clear blue shift of the absorption edge with decreasing thickness is observed. (b) $(\alpha \cdot h\nu)^{1/2}$ representation of the measurements shown in (a). The data is fitted with a linear curve to determine the x-intercept (not shown here), which corresponds to the optical band gap. The inset shows the data for the thickness $d = 1.1$ nm in a double-logarithmic representation. The slopes f = 2 (red) and f = 1/2 (blue) correspond to the indirect and direct absorption gap, respectively.

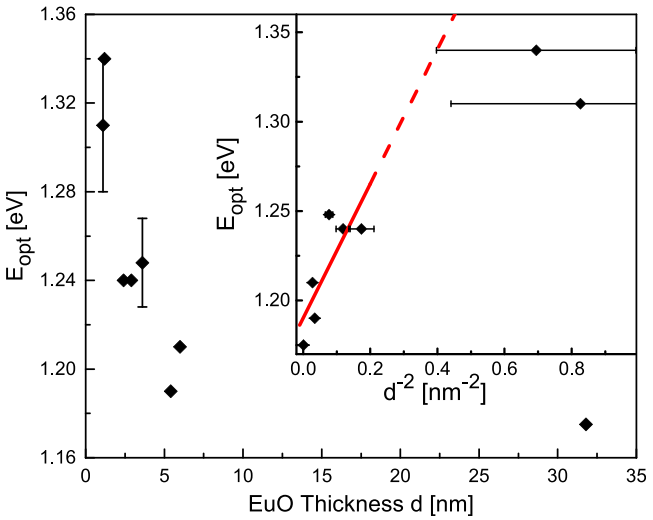

FIG. 4. Dependence of the optical band gap on EuO layer thickness (d between 1.1 nm and 32 nm). Error bars indicate representative statistical errors. The data shows the shift of the optical band-gap energy to higher values for thinner film thickness d. In the inset, the data are plotted against d^{-2} that, in a simple potential well model, leads to a linear dependence. Error bars indicate a monolayer (0.26 nm) deviation of the thickness. The red line is a linear fit to the data. Data points with $d^{-2} > 0.4$ are not included in the fit.

with the energy ($f = 2$ in Eq. (1)) was plotted against the photon energy in Fig. 3(b). To a good approximation, the data show a linear dependence with the axis intercept corresponding to the optical band gap E_{opt}. Deviations at higher energies are due to the fact that Eq. (1) is only valid for a single band and close to the band edge. For thicker samples (e.g., $d = 32$ nm), the data exhibit two linear regions with slightly different slopes. This is commonly observed in the absorption of indirect semiconductors, where different slopes reflect the absorption and emission of phonons, respectively (see, e.g., Refs. 22 and 23). In Fig. 4, the thus determined optical band gap E_{opt} is plotted against the layer thickness. E_{opt} displays a clear blue shift for decreasing EuO layer thickness d, which is most pronounced for small d. This is indicative for a quantum size effect, which—in the simplest model of an infinite square well—shows a $1/d^2$ dependence of the band-gap shift with respect to the bulk value. To test this model, E_{opt} is plotted against $1/d^2$ in the inset of Fig. 4. We find that for all but the thinnest samples ($d = 1.1$ nm and $d = 1.2$ nm), the data falls on a straight line. For $1/d^2 \to 0$, we derive an optical EuO bulk band gap of $E_{opt,bulk} = (1.19 \pm 0.02)$ eV.

There are several possible reasons for the strong deviation from the $1/d^2$-law for the ultrathin layers: First, for high quantization energies, the leakage of the wave function into the barrier region will occur, which reduces the energy with respect to the infinite-well model. Second, carriers high up in the band will not be subject to the same (parabolic) band structure as those close to the band edge. Such non-parabolicity effects increase the effective mass and lead to a further reduction of the quantization energy.[24,25] Third, slight fluctuations of the layer thickness can lead to areas with lower quantization energies, which will somewhat red-shift the absorption data. Because of the $1/d^2$-dependence, this effect will be most prominent in the ultrathin layers.

The linear region of E_{opt} vs. $1/d^2$ (solid red line in the inset of Fig. 4) allows us not only to extrapolate the bulk value of the optical EuO band gap (1.19 ± 0.02 eV) but also to extract information on the EuO band structure, in particular, the effective masses of electrons and holes. Within the infinite-well approximation, the quantization energy $\Delta E(d)$ is given by

$$\Delta E_{e,h}(d) = \frac{h^2}{8 m^*_{e,h} d^2}. \quad (2)$$

Here, m^* is the effective mass of the electron and the hole, indexed by e and h, respectively. The total shift of the absorption edge then follows as

$$\Delta E(d) = \frac{h^2}{8d^2}\left(\frac{1}{m^*_e} + \frac{1}{m^*_h}\right) = \frac{h^2}{8d^2} \cdot \frac{1}{\mu}. \quad (3)$$

The reduced effective mass μ of the optically generated electron hole pair can therefore be deduced from the linear dependence of ΔE on $1/d^2$ in the range $2.4 \le d \le 32$ nm

(see solid red line in the insert of Fig. 4). We find $\mu = (1.0 \pm 0.2)\, m_o$, where m_o is the free electron mass. This value is in good agreement with the longitudinal electron mass in bulk EuO[26] and with the recent experimental[27] and theoretical[28] data of the conduction band dispersion in two-dimensional EuO layers. Note that because the EuO 4*f* valence band has a very weak dispersion[26,29] and the hole mass is correspondingly high, it is expected that $\mu \approx m_e^*$.

In summary, we have investigated all-oxide quantum wells based on the magnetic semiconductor EuO. The excellent single-crystalline layer and interface quality of the YSZ/EuO/MgO heterostructures grown by MBE were confirmed by RHEED, XRD and XRR. Using infrared transmission spectroscopy, we have demonstrated that, independent of the film thickness, the EuO optical band gap is of indirect nature. By varying the thickness of the quantum well layer from bulk-like ($d = 32$ nm) down to the ultrathin film limit ($d = 1.1$ nm), we find a bulk value $E_{opt,bulk} = (1.19 \pm 0.02)$ eV, a blue shift of the EuO absorption edge of up to $\sim$0.2 eV, and a reduced effective mass of the electron-hole pair of $\mu = m_o$. The observed band-gap widening demonstrates the quantum confinement in the fully epitaxial EuO-based oxide heterostructures and provides a route for controlling the band gap in complex oxides for emerging spin- and optoelectronic applications.

We thank R. Pentcheva for inspiring discussions and O. Petracic and the Jülich Centre for Neutronscience for providing measurement time at the SQUID magnetometer. M.M. acknowledges financial support by HGF under Contract No. VH-NG-811.

[1]G. Koster, M. Huijben, and G. Rijnders, *Epitaxial Growth of Complex Metal Oxides* (Elsevier, 2015).
[2]J. Chakhalian, J. W. Freeland, A. J. Millis, C. Panagopoulos, and J. M. Rondinelli, Rev. Mod. Phys. **86**, 1189–1202 (2014).
[3]M. Hoppe, S. Döring, M. Gorgoi, S. Cramm, and M. Müller, Phys. Rev. B **91**, 054418 (2015).
[4]S. Stemmer and A. J. Millis, MRS Bull. **38**, 1032–1039 (2013).
[5]M. Oestreich, J. Hübner, D. Hägele, M. Bender, N. Gerhardt, M. Hofmann, W. W. Rühle, H. Kalt, T. Hartmann, P. Klar, W. Heimbrodt, and W. Stolz, "Spintronics: Spin electronics and optoelectronics in semiconductors," in *Advances in Solid State Physics* (Springer, Berlin, Heidelberg, 2001), pp. 173–186.
[6]A. Mauger and C. Godart, Phys. Rep. **141**, 51–176 (1986).
[7]M. Matsubara, A. Schmehl, J. Mannhart, D. G. Schlom, and M. Fiebig, Phys. Rev. B **86**, 195127 (2012).
[8]M. Müller, G.-X. Miao, and J. S. Moodera, J. Appl. Phys. **105**, 07C917 (2009).
[9]M. Müller, G.-X. Miao, and J. S. Moodera, EPL **88**, 47006 (2009).
[10]G.-X. Miao, M. Müller, and J. S. Moodera, Phys. Rev. Lett. **102**, 076601 (2009).
[11]G. Güntherodt, P. Wachter, and D. M. Imboden, Phys. Kondens. Mater. **12**, 292–310 (1971).
[12]C. Caspers, A. Gloskovskij, W. Drube, C. M. Schneider, and M. Müller, Phys. Rev. B **88**, 245302 (2013).
[13]T. Gerber, P. Lömker, B. Zijlstra, C. Besson, D. N. Mueller, W. Zander, J. Schubert, M. Gorgoi, and M. Müller, J. Mater. Chem. C **4**, 1813–1820 (2016).
[14]C. Caspers, A. Gloskovskii, W. Drube, C. M. Schneider, and M. Müller, J. Appl. Phys. **115**, 17C111 (2014).
[15]R. Sutarto, S. G. Altendorf, B. Coloru, M. Moretti Sala, T. Haupricht, C. F. Chang, Z. Hu, C. Schüßler-Langeheine, N. Hollmann, H. Kierspel, H. H. Hsieh, H.-J. Lin, C. T. Chen, and L. H. Tjeng, Phys. Rev. B **79**, 205318 (2009).
[16]P. Poulopoulos, B. Lewitz, A. Straub, S. D. Pappas, S. A. Droulias, S. Baskoutas, and P. Fumagalli, Appl. Phys. Lett. **100**, 211910 (2012).
[17]J. M. An, S. V. Barabash, V. Ozolins, M. van Schilfgaarde, and K. D. Belashchenko, Phys. Rev. B **83**, 064105 (2011).
[18]P. Liu, J. Tang, J. A. C. Santana, K. D. Belashchenko, and P. A. Dowben, J. Appl. Phys. **109**, 07C311 (2011).
[19]P. V. Lukashev, A. L. Wysocki, J. P. Velev, M. van Schilfgaarde, S. S. Jaswal, K. D. Belashchenko, and E. Y. Tsymbal, Phys. Rev. B **85**, 224414 (2012).
[20]J. A. Colón Santana, J. M. An, N. Wu, K. D. Belashchenko, X. Wang, P. Liu, J. Tang, Y. Losovyj, I. N. Yakovkin, and P. A. Dowben, Phys. Rev. B **85**, 014406 (2012).
[21]V. M. Huxter, T. Mirkovic, P. S. Nair, and G. D. Scholes, Adv. Mater. **20**, 2439–2443 (2008).
[22]P. M. Yu and M. Cardona, *Fundamentals of Semiconductors* (Springer, 2001).
[23]G. G. Macfarlane and V. Roberts, Phys. Rev. **97**, 1714–1716 (1955).
[24]U. Ekenberg, Phys. Rev. B **40**, 7714–7726 (1989).
[25]C. Wetzel, R. Winkler, M. Drechsler, B. K. Meyer, U. Rössler, J. Scriba, J. P. Kotthaus, V. Härle, and F. Scholz, Phys. Rev. B **53**, 1038–1041 (1996).
[26]S. J. Cho, Phys. Rev. B **1**, 4589–4603 (1970).
[27]J. Klinkhammer, M. Schlipf, F. Craes, S. Runte, T. Michely, and C. Busse, Phys. Rev. Lett. **112**, 016803 (2014).
[28]R. Schiller and W. Nolting, Phys. Rev. Lett. **86**, 3847–3850 (2001).
[29]H. Miyazaki, T. Ito, H. Im, S. Yagi, M. Kato, K. Soda, and S. Kimura, Phys. Rev. Lett. **102**, 227203 (2009).